

Evaluation of Carrier Density and Gain Profile in a Semiconductor Laser

H. Golnabi¹

In this paper, a precise method for computing the optical gain/loss in an optically pumped semiconductor material is reported. Variations of the gain coefficient, as a function of pump light frequency for different band gap energies, temperature and carrier densities, are described. In another study, variations of the electron and hole densities are simulated and the resulting integrals are evaluated numerically. The changes of carrier density in an intrinsic GaAs semiconductor as a function of the position of the quasi-Fermi levels in the conduction or valence bands for different temperatures, are also reported. For GaAs laser, accurate normalized densities are obtained as a function of temperature. The normalized densities at $T = 300^\circ\text{K}$ are at the ratio of 1.98:1:0.4 for $T = 200, 300$ and 400°K , respectively. The peak gain values, normalized at the same room temperature, are at the ratio of 2.05:1:0.36, for $T = 200, 300$ and 400°K , respectively. Comparing the results presented for the carrier density and gain, with other studies, this method provides an accurate result. It is noted that temperature has a dominating effect on the gain profile and, as a result, on the laser overall performance as observed in the experiments.

INTRODUCTION

In recent years, many applications have been found for semiconductor lasers in the field of electro-optics, communication, optical pumping and control systems [1-3]. Developing efficient laser systems demands devices with a high gain and good beam quality which require a low injection current. To reach a high performance, advances are made in theoretical aspects and the related manufacturing techniques [4]. As a result, considerable achievements have been made in this field both theoretically and experimentally. Different design geometries and structures have been developed in recent years.

An important issue in optical amplification has been the problem of population inversion and the gain coefficient in such a medium. To understand the physics of laser operation, density of the states, transition probability and stimulated emission are studied extensively in semiconductor materials prepared by homojunction and heterojunction methods. However, there are a few points which still need more attention in optimizing such devices. For example the role of band gap variation, induced light energy and carrier density for better performance must be reconsidered. The aim

of this study is to simulate such a device and provide useful information which can be implemented in design and fabrication of such optical amplifiers.

To study the gain in a semiconductor material experimentally, a strong optical pump for creating an inversion by moving the quasi-Fermi levels into the bands is required. In this method, the net gain can be measured by monitoring the input and output probe beam coming out of the slab material under study [5]. This study can provide useful information concerning the gain in terms of the pump beam criteria and the semiconductor material for such amplifiers. In the case of laser operation the direct bias voltage, instead of the optical pumping, accomplishes the inversion. For the semiconductor laser, the theory of the interaction of light with matter is used and for such a device the gain must be studied.

THEORY

In this analysis, the semiconductor model is considered to have an upper-level (conduction band), where electrons can flow and a lower-level (valence band), where the holes can flow. If an electron of momentum $+\hbar\mathbf{k}$ (\hbar , Dirac constant and \mathbf{k} , wave vector) in the valence band absorbs light, it is excited into the conduction band, leaving behind a hole of momentum $-\hbar\mathbf{k}$ in the valence band. The energy of the photon inducing this

1. Institute of Water and Energy, Sharif University of Technology, P.O. Box 11365-8639, Tehran, I.R. Iran.

transition is given by:

$$\begin{aligned}\hbar\omega(\mathbf{k}) &= \varepsilon_e(\mathbf{k}) + \varepsilon_h(\mathbf{k}) + Eg + \delta Eg \\ &= \varepsilon(\mathbf{k}) + Eg + \delta E_g,\end{aligned}\quad (1)$$

where ε_β (β can be e or h for electron or hole, respectively) is the reduced-mass energy related to the carrier and the total reduced-mass energy ε is related to the momentum by:

$$\varepsilon(\mathbf{k}) = (\hbar^2\mathbf{k}^2)/2m_r, \quad (2)$$

where m_r is the reduced mass defined by Equation 6. In Equation 1 Eg is the zero-field band gap energy and δE_g is a reduction term in the band gap energy due to the interband electron-electron and hole-hole coulomb and the fermions exchange correlation. Interaction with electron-hole coulomb attraction can be important for low carrier densities. Such coulomb attraction can create excitations, which are similar to an H-like atom, consisting of a bound electron-hole pair. For instance, the excitation Bohr radius in GaAs is 1243 nm and the excitation Rydberg energy is approximately 4.2 meV. This is small compared to 13.6 eV for the H atom and also to the room temperature energy of 25 meV.

According to [5], the gain equation for a typical semiconductor laser is as follows:

$$\gamma(\nu) = B_{21}(h\nu)(n_g/c)\rho_{\text{red}}(h\nu)[f_c(E_b) - f_v(E_a)], \quad (3)$$

where $B_{21}(h\nu)$ is the quantity which determines the transition rate of the electron between the upper and lower levels in the presence of radiation. The second coefficient is the inverse of the group velocity and $\rho_{\text{red}}(h\nu)$ is the density of carriers which can participate in the amplification process. Function $f_c(E_b)$ gives the occupation probability distribution of electron state b with energy E_b in the conduction band and $f_v(E_a)$ shows the occupation probability function for the hole state, E_a , in the valence band. The difference of these two probability functions, reported in Equation 3, shows the net occupation probability of the electronic upper state and the vacancies in the lower state.

The transition probability is defined as in [6]:

$$\begin{aligned}B_{21}(h\nu) &= [e^2h/(6m_e\varepsilon_0n_g^2)][(1 + \Delta/E_g)/ \\ &(1 + 2\Delta/3E_g)](1 - m_e/m_0),\end{aligned}\quad (4)$$

where e is the electron charge, h the Planck constant, ε_0 the free space permittivity, E_g the band gap energy, m_e the effective mass of the electron and n_g the effective index of refraction (3.75 for GaAs). Here Δ is the spin-orbit coupling (0.33 eV for GaAs). The third term $\rho_{\text{red}}(h\nu)$ is the density of state per energy interval dE which can participate in the photonic process given by:

$$\rho_{\text{red}}(h\nu) = 1/(4\pi^2)(2m_r/\hbar^2)^{3/2}(h\nu - E_g)^{1/2}, \quad (5)$$

Therefore, m_r is the reduced mass determined from:

$$m_r = m_e m_h / (m_e + m_h), \quad (6)$$

where m_h is the hole effective mass ($m_h = 0.55 m_0$ and $m_e = 0.067 m_0$ for GaAs semiconductor).

Finally, the last term in Equation 3, which gives the net rate of stimulated transitions can be found as follows: First, it is necessary to define the energy of states E_a and E_b in the respective bands and then using quasi-Fermi levels, one can define $f_c(E_b)$ and $f_v(E_a)$. Considering [5], the following can be written:

$$E_b = E_c + [m_h/(m_e + m_h)](h\nu - E_g), \quad (7a)$$

$$E_a = E_v - [m_e/(m_e + m_h)](h\nu - E_g). \quad (7b)$$

Thus, the occupation probability functions are:

$$f_c(E_b) = [1 + \exp(E_b - F_n/kT)]^{-1}, \quad (8a)$$

$$f_v(E_a) = [1 + \exp(F_p - E_a/kT)]^{-1}, \quad (8b)$$

where F_n and F_p are the quasi-Fermi levels and k is the Boltzmann constant. To determine these levels, a fixed temperature ($T = 0^\circ\text{K}$) is assumed, then the injected density of carriers are known at that particular temperature and hence, the following can be written:

$$F_n = E_c + \hbar^2/(2m_e)(3\pi^2 n)^{2/3}, \quad (9a)$$

$$F_p = E_v - \hbar^2/(2m_h)(3\pi^2 p)^{2/3}, \quad (9b)$$

where n and p show the electron and hole density, respectively. The temperature dependence of n and p is discussed in the next section. Therefore, with these equations in hand, the gain variation as a function of different parameters has been studied.

In the next section, the variation of the electron and hole densities as a function of the related parameters is considered. Following analysis given in [5], it can be written that:

$$\begin{aligned}n &= 1/(2\pi^2)[2m_e/\hbar^2]^{3/2} \int (\varepsilon - E_c)^{1/2} d\varepsilon / \\ &\{\exp[(\varepsilon - F_n)/kT] + 1\},\end{aligned}\quad (10a)$$

$$\begin{aligned}p &= 1/(2\pi^2)[2m_h/\hbar^2]^{3/2} \int (E_v - \varepsilon)^{1/2} d\varepsilon / \\ &\{\exp[(F_p - \varepsilon)/kT] + 1\},\end{aligned}\quad (10b)$$

where in Equation 10a integration is from E_c to infinity and in Equation 10b is from zero to E_v . To evaluate these quantities, substitutions $\varepsilon = E_c + u$ and $\varepsilon = E_v - u$ in Equations 10a and 10b are made and the following are identified:

$$x = u/kT, \quad (11a)$$

$$a = \exp\{[F_p - E_v]/kT\}, \quad (11b)$$

$$b = \exp\{[E_c - F_n]/kT\}, \quad (11c)$$

where a , b and x are all dependent on energy and temperature. Considering the above substitutions the following are obtained:

$$n = 1/(2\pi^2)[2m_e kT/\hbar^2]^{3/2} \left\{ \exp - [(E_c - F_n)/kT] \right\} \int x^{1/2} dx / (e^x + 1/b), \quad (12a)$$

$$p = 1/(2\pi^2)[2m_h kT/\hbar^2]^{3/2} \left\{ \exp - [(F_p - E_v)/kT] \right\} \int x^{1/2} dx / (e^x + 1/a), \quad (12b)$$

where integration on x is from zero to infinity. For the case of $(a, b) \gg 1$, the integral in Equation 12 can be evaluated in closed form which results in $\pi^{1/2}/2$. This is a good approximation for semiconductor electronics such as transistors and diodes, in which the Fermi levels are in the gap and thus factors a and b are much greater than one. If a semiconductor was in equilibrium so that $F_n = F_p = E_f$, then the product of n and p would yield a constant which depends on the gap energy $E_c - E_v = E_g$, temperature and effective masses in the bands, but not on the position of the Fermi levels.

However, a semiconductor laser is not a system in equilibrium; furthermore, the replacement of the denominators of Equations 12 by the exponential is not valid because at least one of the quasi-Fermi levels must be in a band for an inversion and thus (a, b) may be less than one. Hence, the integral of the form:

$$I = 2/\pi^{1/2} \int x^{1/2} dx / [e^x + 1/(a, b)], \quad (13)$$

must be evaluated numerically. To evaluate this integral, three approximations are considered. In the first case, an integration range of zero to 100 instead of zero to infinity is assumed. In the second case, to evaluate this integral $y = x/(x + 1)$ is assumed, thus this integral becomes:

$$I = \int y^{1/2} dy / \{(1 - y)^{3/2} [e^{y/(1-y)} + K]\}, \quad (14)$$

where integration is from zero to one and $K = 1/(a, b)$ for hole and electron states, respectively. Finally, in the third approximation the variable $y = 1/(x + 1)$ is used and the resulting integral evaluated.

The gain formula given in Equation 3 is analogous to the gain for the conventional lasers and provides a good means for comparison. However, in order to have a better view of the gain, the gain function $\alpha(\nu, T)$ from the expression based on the interaction of light and matter described in [7,8] is considered as:

$$\alpha = A \int \varepsilon^{1/2} \{ [1 + (\varepsilon - \delta)^2/\gamma^2]^{-1} \{ f_e(\mathbf{k}) + f_h(\mathbf{k}) - 1 \} \} d\varepsilon, \quad (15)$$

where integration is from zero to infinity and A is a constant defined by:

$$A = \nu \varphi^2 / [2\mathcal{E} \hbar \gamma (2\pi^2 a_o^3 E_R^{3/2})], \quad (16)$$

a_o is the excitation Bohr radius and E_R Rydberg energy is given by:

$$a_o = \hbar^2 \varepsilon / (m e^2), \quad (17)$$

$$E_R = \hbar / (2m a_o), \quad (18)$$

and \mathcal{E} is the permittivity of the medium. γ is usually given in terms of its inverse, the carrier-carrier scattering time ($\gamma = 1/\tau$). In Equation 16 ν is the angular laser oscillation frequency and parameter φ is defined in [8]. In terms of the reduced-mass energy, ε , the energy detuning (difference between the induced and laser photon energies) is:

$$\hbar(\omega - \nu) = \varepsilon - \hbar\delta, \quad (19)$$

where $\hbar\delta$ is laser detuning and, relative to the renormalized band gap, is given by (using Equation 1):

$$\hbar\delta = \hbar\nu - E_g - \delta E_g. \quad (20)$$

For a semiconductor laser α , given in Equation 15 must be positive. For simplicity if the linewidth function is assumed to be a Dirac-function, gain occurs for $f_e + f_h - 1 > 0$, which according to Equations 21 means that the electron-hole plasma should have a population inversion. Thus, if the gain exceeds the cavity losses, laser action can occur.

It must be noted that both the carrier density functions f_e and f_h are functions of the reduced-mass energy, ε , 0 and temperature. The carrier (electron/hole) probability functions are:

$$f_e = 1 / \{ \exp[\beta(\varepsilon/m_e - \mu_e)] + 1 \}, \quad (21a)$$

$$f_h = 1 / \{ \exp[\beta(\varepsilon/m_h - \mu_h)] + 1 \}, \quad (21b)$$

where $m_\kappa = m_\kappa/m$ (κ can be e or h) is the effective mass ratio, used for the electrons and holes, respectively and $\beta = 1/kT$. Parameter μ_β (μ_e and μ_h) in Equations 21 is the carrier chemical potential, which is chosen to yield the total carrier density N . Quasi-Fermi level and chemical potential are taken as synonyms (compare Equations 21 and 8). However, as discussed before, using chemical potential consideration, the reduced-mass energy and reduced-mass notations like H-atom are used due to the $e - e$ and $e - h$ interactions. From Equations 21, it can be seen that μ_β equals the carrier energy, ε_β , for which f_β is precisely one half. This chemical potential depends on the material temperature and is decreased, as the temperature is increased. The chemical potentials are

chosen so that the total carrier number density, N , for all temperatures remains constant. The value of this parameter is positive for electron while it is negative for hole. The total chemical potential $\mu_e + \mu_h$ is a crucial parameter in semiconductor laser theory since it defines the upper limit of the gain region similar to $(F_n - F_p)$ limit. It can be shown that the inversion is achieved if the reduced-mass energy, ε , obeys the relation $0 < \varepsilon < \mu_e + \mu_h$.

RESULTS

For the first study, a simple program is arranged to compute and plot the gain coefficient given in Equation 3 for GaAs semiconductor. Figure 1 shows this gain as a function of the induced light frequency (photon energy) at various temperature. The temperature value is changed from $T = 95^\circ\text{K}$ to 305°K . As shown in Figure 1, when temperature decreases, the gain increases; for the highest temperature in Figure 1, gain is approximately $1 \times 10^5 \text{ m}^{-1}$. Any increase in temperature will decrease the gain, which is around $0.55 \times 10^5 \text{ m}^{-1}$ at $T = 305^\circ\text{K}$. Similarly one can see the absorbing loss factor of the GaAs material for the same temperature change as shown in the same figure.

As temperature is changed, the loss changes in magnitude and profile. For $T = 95^\circ\text{K}$, the loss is at minimum, while at $T = 305^\circ\text{K}$, it is at highest. The gain curve grows at the induced light frequency, corresponding to gap energy of $E_g = E_c - E_v$. For the frequency value corresponding to energy of $F_n - F_p$ it reaches zero and at higher induced light frequencies there is loss instead of gain in the semiconductor. For $T = 0^\circ\text{K}$, the gain reaches zero very sharply, while

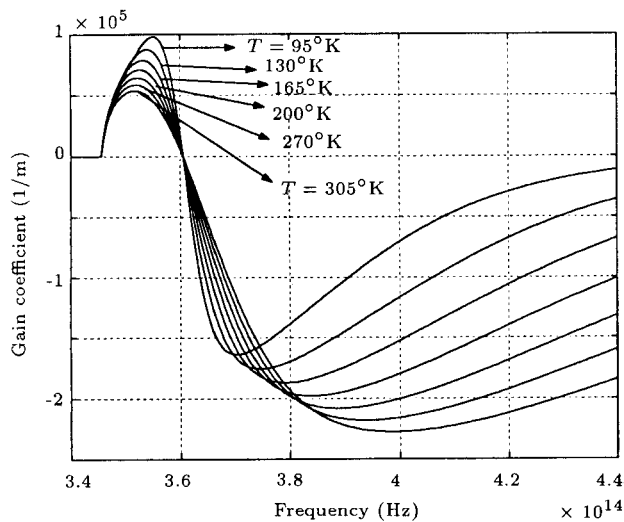


Figure 1. Optical-gain (loss) variation as a function of pump light frequency for GaAs semiconductor at different temperatures. The injected carrier density is assumed to be $n=p=1 \times 10^{18} \text{ cm}^{-3}$ and band gap energy $E_g=1.43 \text{ eV}$.

at higher temperatures the decrease is at slower rate (Figure 1). Also, as the temperature increases, the gain profile gets wider and the gain bandwidth increases and it is minimum for $T = 95^\circ\text{K}$. A similar feature is noted for the loss profile as can be seen in Figure 1.

The dependence of optical gain in GaAs on frequency and injected carrier density is presented in Figure 2. The injected carrier density was changed from 1×10^{18} to $3 \times 10^{18} \text{ (cm}^{-3}\text{)}$ and the results were compared. As the carrier density was increased, the gain coefficient was increased correspondingly. Using a similar approach, Vahala et al. [9] calculated the dependence of optical gain in a GaAs $p-n$ junction on frequency and injected carrier density. Casey and Stern [10] gave absorption and spontaneous emission for such a material. The peak value of the gain for such laser is approximated as:

$$\gamma_{\max} = B_g(N_{\text{inj}} - N_{\text{th}}), \quad (22)$$

where $B_g = 1.5 \times 10^{-16} \text{ cm}^2$ at $T = 300^\circ\text{K}$ and $B_g = 5 \times 10^{-16} \text{ cm}^2$ at 77°K . N_{inj} is the injection carrier density in cm^{-3} and N_{th} is approximately $1.55 \times 10^{18} \text{ cm}^{-3}$ (see [11]).

Recent articles in the literature have focused on the single or Multiple Quantum-Well (MQW) lasers and discussed the gain for different materials and geometries [12,13]. The final form of the gain for a bulk semiconductor or quantum well material is given as a function of the injected current density, rather than carrier density. However, carrier density is of great importance to the proper design and optimization

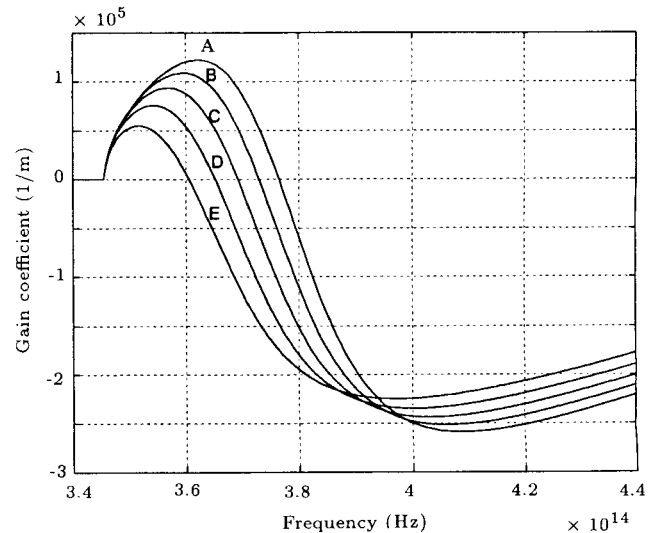


Figure 2. Variation of optical gain (loss) in GaAs versus pump light frequency and injected carrier density. Curves from top to bottom show carrier density of $A=3 \times 10^{18}$, $B=2.5 \times 10^{18}$, $C=2 \times 10^{18}$, $D=1.1 \times 10^{18}$ and $E=1 \times 10^{18} \text{ cm}^{-3}$. The temperature is assumed to be 295°K and the band gap energy $E_g = 1.43 \text{ eV}$.

of semiconductor lasers. Many publications have been devoted to theoretical gain calculation, but as indicated in [14] there are still some inconsistencies for gain expression in GaAs. For MQW lasers the expression for gain and spontaneous emission in semiconductors has been written within the framework of Fermi Golden Rule. Within this frame work, the major components of gain calculations are the electron, hole density of state and the transition matrix element describing the interaction between the conduction and valence band states. In such analysis they calculated the magnitude of the momentum matrix elements.

In Figure 3, the effect of the band gap energy on the gain (loss) profile is considered. Here, this parameter varies from 1.40 to 1.45 eV (E_g for GaAs is about 1.436 eV) and the results are plotted. As can be seen in this figure, the gain coefficient is less sensitive to this variation and a minor change in the band gap energy does not have a noticeable effect on the gain (loss) magnitude. The carrier density here is assumed to be $1.2 \times 10^{18} \text{ cm}^{-3}$ and temperature is $T = 295^\circ\text{K}$. Also, as noted in Figure 3, the gain energy range and the threshold pump energy are determined from the relation such as $F_n - F_n > h\nu > E_g$.

To evaluate the integral (Equation 14) in Figure 4, the density integral is shown as a function of the integral variable x for different $K(1/a, b)$ values. Parameters a and b show the position of the quasi-Fermi level in the valence and conduction bands, respectively. As mentioned in the first approximation, this integral is calculated for the range of 0 to 100 and for higher x values is close to zero. Curve A corresponds to

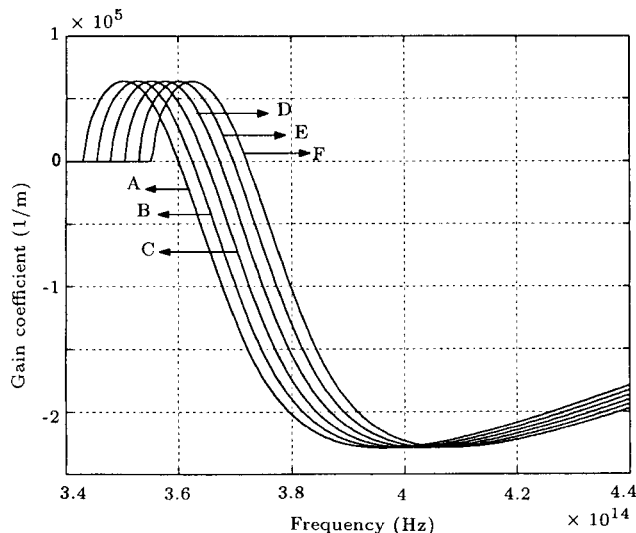


Figure 3. Dependence of optical-gain (loss) in GaAs on pump light frequency and band gap energy. Curves from left to right correspond to band gap energy of $E_g=1.40$ (A), 1.41(B), 1.42(C), 1.43(D), 1.44(E) and 1.45 eV (F), respectively. Here $T = 295^\circ\text{K}$ and carrier density $n = p = 1.2 \times 10^{18} \text{ cm}^{-3}$.

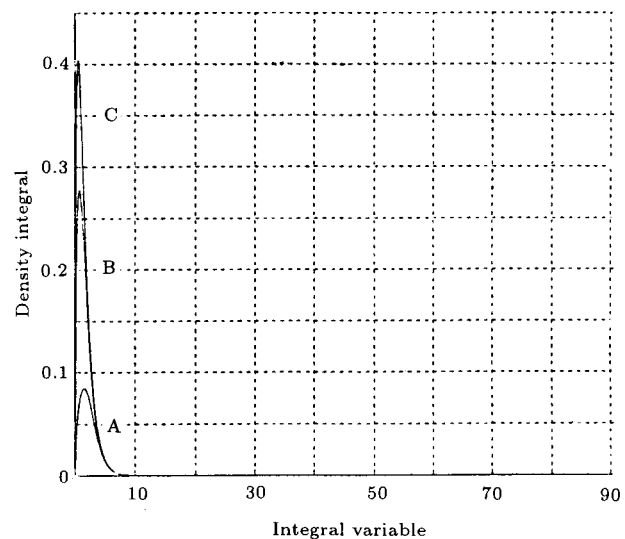


Figure 4. Density integral as a function of the integral range for the first approximation for different K values. Curve marked A shows $(a, b) = 0.1$, curve B is for $(a, b) = 1$ and curve C shows results for $(a, b) = 10$.

$(a, b) = 0.1$ (Fermi levels within bands), B to $(a, b) = 1$ (Fermi levels just at the edge of the related bands) and curve C represents the results for $(a, b) = 10$ (Fermi levels in gap). It must be pointed out that this integral has a limiting value of $I = \pi^{1/2}/2 = 0.88$ when the effect of K in the denominator of Equation 14 is ignored. Increasing (a, b) value increases the integral value; curve A has a larger value than B while curve C has the smallest value. Only curve A satisfies the laser condition. Also as (a, b) is increased, $1/(a, b)$ gets smaller and as it reaches infinity the integral value approaches the limiting value of 0.88. For the case of both $(a, b) \gg 1$, the quasi-Fermi levels always are in gap, which does not meet the laser condition and at least one of the Fermi levels should be within bands.

The result of the third approximation for new variable y is plotted in Figure 5. In this computation y is defined to be $1/(1+x)$ and the range of integration for y is from zero to unity. The density integrals for different K values as mentioned before are presented in this figure. As (a, b) increases, the density integral increases. It is noted that there is a y value that maximizes the integral value and the peak of the density function shifts to higher y values as parameter (a, b) is increased. Similar to Figure 4, as the (a, b) value is increased, the density function becomes more spread. The physical importance of the variations of K and integral variables x or y can be seen from Equation 9. Parameter u shows the energy variation and x demonstrates the ratio of this energy change to the kT values. Therefore, x shows the height of the density integral and (a, b) , depending on the Quasi-Fermi level energies, displays the spreading of the function. If the density integral is multiplied by

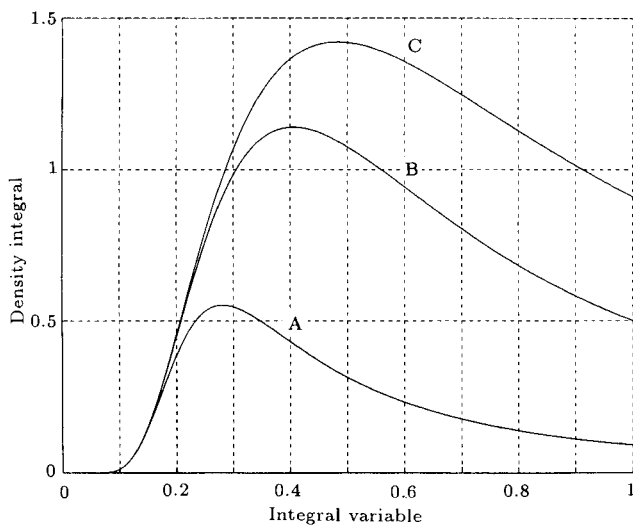


Figure 5. Density integral as a function of the integral range for the third approximation for different K values. The curve marked A shows $(a, b) = 0.1$, curve B is for $(a, b) = 1$ and curve C shows results for $(a, b) = 10$.

a constant (see Equation 10), the carrier density is obtained at a particular temperature.

In the first part the electron density for different temperature ranges of $T = 100, 200, 300$ and 400°K was computed. Figure 6 shows the electron density in an intrinsic GaAs semiconductor as a function of the position of the quasi-Fermi level b for different approximations. Positive energy corresponds to the position of the quasi-Fermi level in the conduction

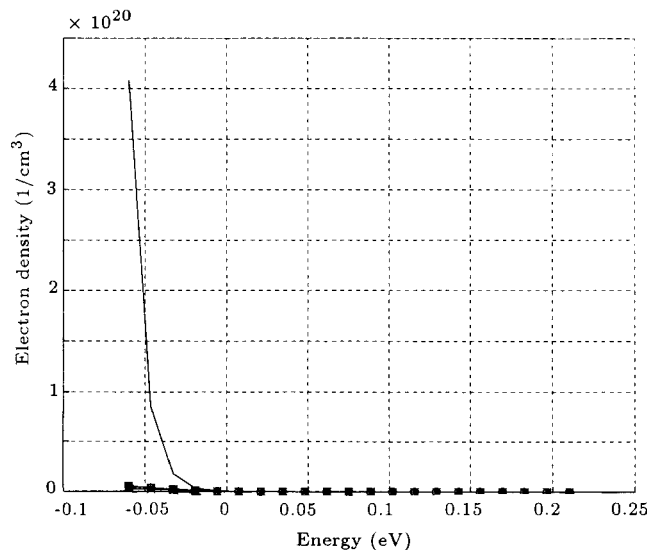


Figure 6. Electron density in an intrinsic GaAs as a function of the position of the quasi-Fermi level b in the conduction band for different cases at temperature of $T = 100^\circ\text{K}$. The solid line shows the resulting density for assuming $I = \pi^{1/2}/2 = 0.88$. Curves denoted by square, star and cross symbols show the results for the three approximations, respectively.

band for electron, while the negative energy value corresponds to the position within the forbidden band gap. Similar comments apply to the valence band for the hole and at zero energy these levels are just at the edge of the respected bands. The energy range is from -0.06 eV to 0.21 eV, which covers the whole range of the possible Fermi level in the band energy diagram. The solid line shows the results for assuming density integral equal to $I = \pi^{1/2}/2 = 0.88$. Other curves denoted by different symbols correspond to the results of the three approximations described above. It is noted that at low temperatures, the three approximations provide similar results. Here the electron density for energies above or below the conduction band is considered. The electron number density rapidly decreases towards the higher energies above the conduction band edge. However, the electron density at such lower temperature peaks for the solid curve while for other cases it is negligible.

Increasing temperature decreases the electron density and the results for $T = 300^\circ\text{K}$ are shown in Figure 7. Comparing these results with those of Figure 6 for $T = 100^\circ\text{K}$, two points can be made. First, as mentioned above, the number density is reduced by a factor of 200. Second, the results for the limiting case and approximations show a considerable difference. However, the first (square) and second (star) cases show almost the same results, while the third approximation provides a lower electron density (denoted by cross) below the conduction edge. At

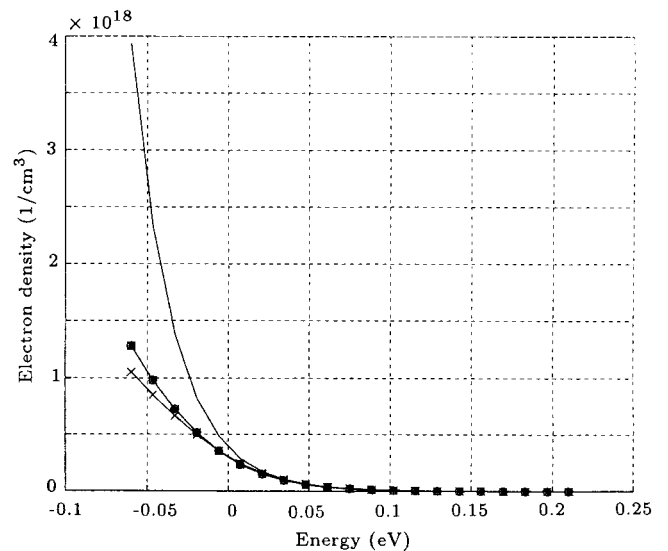


Figure 7. Electron density in an intrinsic GaAs as a function of the position of the quasi-Fermi level b in the conduction band for different cases at temperature $T = 100^\circ\text{K}$. The solid line shows the resulting density for assuming $I = \pi^{1/2}/2 = 0.88$. The curves denoted by square, star and cross symbols show the results for the three approximations, respectively.

energies higher than the conduction, all the results overlap with each other as shown in Figure 7.

A similar study is performed for the hole density and Figure 8 shows this result for $T = 300^\circ\text{K}$. For a better comparison, densities were plotted for both cases at similar temperatures. As can be seen in Figure 8, a similar feature is observed for the hole density as a function of the variation for the quasi-Fermi level energies in the valence band for different temperatures. If the result of this figure are compared with that of Figure 7 for electron density, it can be observed that the hole density is higher by a factor of 23.5, which is expected from the effective mass ratio.

Important physical inter-operations are as follows. Considering Figures 7 and 8, the electron and hole densities are very strong functions of lattice temperature, T . Compare Figures 6 and 7 for electron densities at different temperatures. Also the difference between the electron and holes density functions is noteworthy. For example from Figure 7, at room temperature, $T = 300^\circ\text{K}$, it takes approximately 3.3×10^{17} electrons/cm³ to move the quasi-Fermi level for electrons to the edge of the conduction band (energy zero in Figure 7). According to Figure 8, it takes 0.735×10^{19} holes/cm³ (23.5 times as many as electrons) to make $F_p = E_g$ (move the quasi-Fermi level to the edge of the valence band corresponding to zero energy in Figure 8). Therefore, it is suggested that electrons should be created or injected into a region which is heavily doped p -type. The physical reason is that electrons are lighter

than holes and the number given corresponds to the ratio of effective masses for two carriers (about 23.5).

For equal electron and hole densities (steady state, say 1.27×10^{18} holes/cm³, the quasi-Fermi level for the electrons is inside the conduction band ($[E_c - F_n]/kT = -2.05$, $E_c - F_n = -0.05$ eV at $T = 300^\circ\text{K}$), where the quasi-Fermi level for the holes is still in the forbidden gap ($[F_p - E_v]/kT = 2.05$, $F_p - E_v = 0.05$ eV); however, the difference $F_n - F_p$ equals the band gap $E_g = 1.436$ eV. The necessary condition for amplification is that a pumping mechanism creates an inversion expressed by the $F_n - F_p > h\nu > E_g$ inequality. Therefore, if one pumps harder to meet this condition and to create more electron-hole pairs, one obtains net optical gain.

The results reported show the gain at fixed values of the electron and hole densities. As described in Equations 12, these densities are variable and changing with parameters such as energy, temperature and the effective reduced masses. Now the next question is how do n and p vary with respect to these parameters? To answer this, the exact integration of Equations 12 has to be considered. Since the effective masses only change the results by a constant factor, the effect of temperature and energy is considered in evaluating such integrals.

In order to check the reported density functions with the numerical evaluations, the normalized functions as given in [8] were considered. The function which appears in integral of Equation 15 is $\varepsilon^{1/2}d_o(\mathbf{k}) = \varepsilon^{1/2}[f_e(\mathbf{k}) + f_h(\mathbf{k}) - 1]$, so normalized densities are represented as $\varepsilon^{1/2}f_e$, $\varepsilon^{1/2}f_h$ and $\varepsilon^{1/2}d_o$. In this way the numbers can be compared precisely. Figures 6 to 9 of that report show the density of electron $\varepsilon^{1/2}f_e(\mathbf{k})$ (vertical axis), holes $\varepsilon^{1/2}f_h(\mathbf{k})$ and all $\varepsilon^{1/2}d_o(\mathbf{k})$ in units of $(2\pi)^2 E_R$ versus reduced energy ε in meV for $T = 300^\circ\text{K}$.

To evaluate the gain, it is necessary to know the Fermi-Dirac distributions for the electrons and holes to be used in Equation 15. The normalized probability distributions as a function of the reduced-mass energy ε are shown in Figure 9. The solid line shows the normalized electron probability function $\varepsilon^{1/2}f_e(\mathbf{k})$, the dashed line shows hole probability $\varepsilon^{1/2}f_h(\mathbf{k})$ and the dot-dashed line shows the function $\varepsilon^{1/2}d_o(\mathbf{k})$. All functions in the units of $(2\pi)^2 E_R$ versus the reduced-mass energy ε are in meV. Here it is assumed that $T = 300^\circ\text{K}$, a carrier density is 3.5×10^{18} carriers/cm³, $a_o = 1.243 \times 10^{-6}$ cm and $E_R = 4.2$ meV. Where $m_e/m = 1.127$, $m_h/m = 8.82$, $\mu_e = 4.73kT$ and $\mu_h = -0.86kT$. In Figure 9, the distribution of this function versus the reduced-mass energy is obtained and is similar to the result provided in [8,11]. It is noted that each distribution has a maximum value at a particular ε value. For the given conditions f_e is maximum at ε about 80, f_h at about 150 and

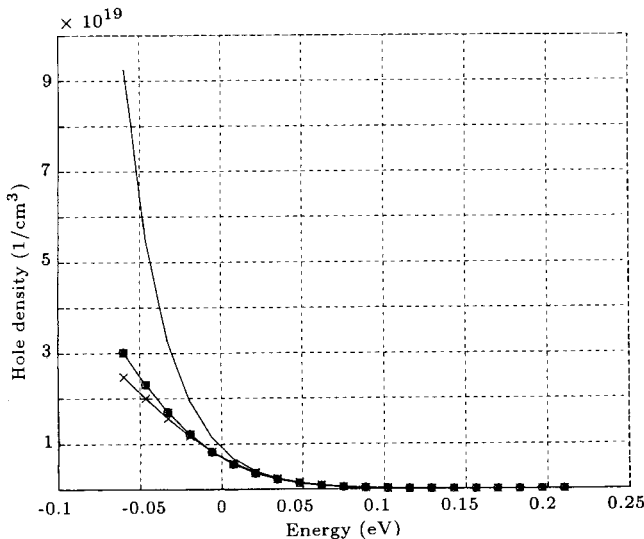


Figure 8. Hole density for the GaAs material as a function of the position of the quasi-Fermi level a in the valence band for different cases at temperature of $T = 300^\circ\text{K}$. The solid line shows the resulting density for assuming $I = \pi^{1/2}/2 = 0.88$. The curves denoted by square, star and cross symbols show the results for the three approximations, respectively.

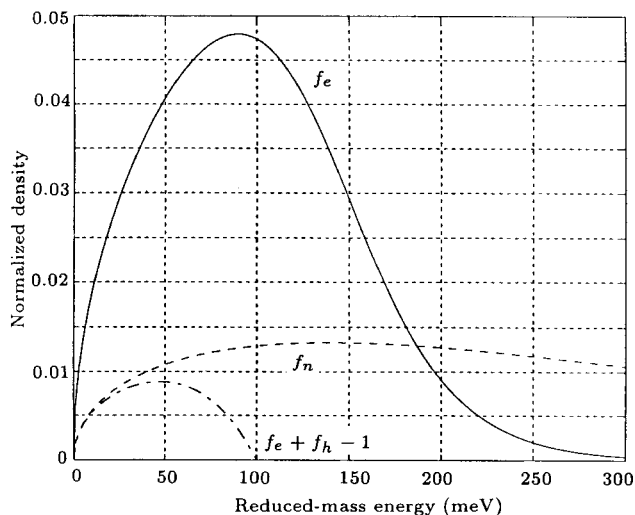


Figure 9. The normalized distribution function as a function of the reduced-mass energy ε . The solid line shows $\varepsilon^{1/2}[f_e(\mathbf{k})]$, the dashed line shows $\varepsilon^{1/2}[f_h(\mathbf{k})]$ and the dot-dashed line shows the $\varepsilon^{1/2}d_o(\mathbf{k})$ all in the units of $(2\pi)^2 E_R$ versus ε in meV. Here $T = 300^\circ\text{K}$ and a carrier density of 3.5×10^{18} carriers/cm³, $a_o = 1.243 \times 10^{-6}$ cm and $E_R = 4.2$ meV, where $m_e/m = 1.127$, $m_h/m = 8.82$, $\mu_e = 4.73$ kT and $\mu_h = -0.86$ kT.

probability difference d_o at about 50. In this figure, in order to obtain the real carrier density f_e and f_h , one must multiply these numbers on the vertical axis by a factor of $[(2\pi)^2 E_R]/\varepsilon^{1/2}$ (compare Figure 9 with Figures 6 to 9 of [8]).

Similarly in Figure 10, density function is defined as $\varepsilon^{1/2}d_o(\mathbf{k}) = \varepsilon^{1/2}[f_e(\mathbf{k}) + f_h(\mathbf{k}) - 1]$ (vertical axis) versus reduced-mass energy, ε . Figure 10 shows the normalized density function for a GaAs laser as a function of the reduced-mass energy for different temperatures. The real density difference d_o can be obtained by multiplying the given numbers on the vertical axis by factor $[(2\pi)^2 E_R]/\varepsilon^{1/2}$, for that specific reduced-mass energy. Other parameters are the same as before, except T which is changed in this study. A comparison of Figure 10 with Figures 6 to 10 of [8] indicates the validity of the computed results.

To define the gain function expressed in Equation 15, this function is plotted for the GaAs semiconductor laser. Figure 11 shows this gain profile as a function of the detuning energy for three different temperatures. Other parameters are the same as before, described in Figures 9 and 10, except T which is changed in this study. In Figure 11, the gain, α , (vertical axis) is shown versus detuning energy, $\hbar\delta$, for different temperatures. Numbers on the vertical axis given for the gain can be obtained by multiplying by a constant related to A , as defined in Equation 16. As seen in Figure 11, an increase in temperature reduces the gain by spreading the carriers out. This spreading is because of the carrier density, as seen in Figure 6,

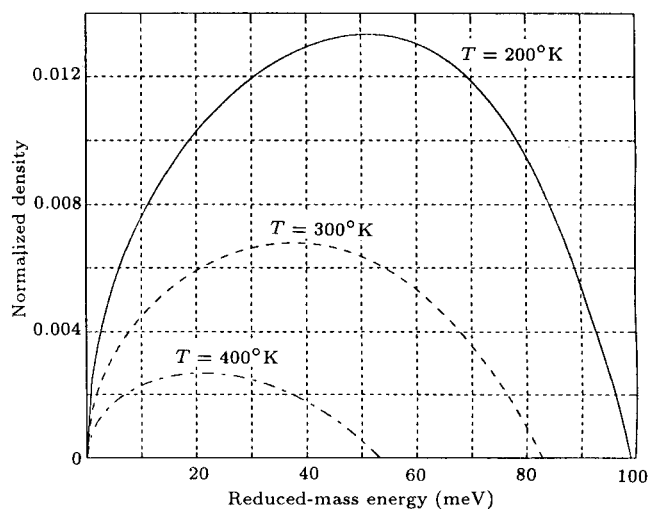


Figure 10. The normalized density function for a GaAs laser as a function of the reduced-mass energy for different temperatures. The plotted function is $\varepsilon^{1/2}d_o(\mathbf{k})$. The real density can be obtained by multiplying the given numbers by factor $[(2\pi)^2 E_R]/\varepsilon^{1/2}$. Other parameters are the same as before and T is changed in this study.

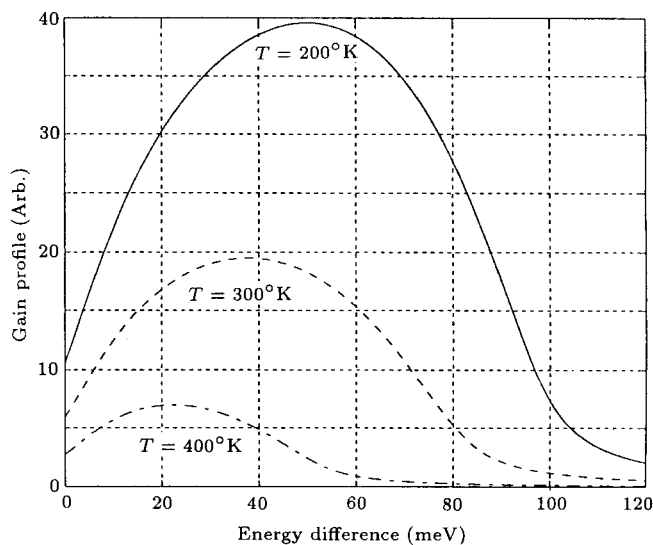


Figure 11. The normalized gain profile as a function of the detuning energy ($\hbar\delta$) for different temperatures in a GaAs laser. The gain values can be found by multiplying the given numbers by a factor of A defined in Equation 16. Other values are the same as before for the GaAs laser.

which shows this variation for the electron density function. Furthermore, Figure 11 is compared with Figures 5-7 presented in [11]. The peak gain values and distributions obtained in this study are consistent with that report. It must be pointed out that other parameters chosen were also the same. This manifests the validity of the reported numerical results.

As discussed, F_n shows the probability of a state being filled in the conduction band and F_p illustrates the probability that a state in the valence band is filled.

Hence, the probability of an empty state (hole state) is $1 - f_{c,v}$ for each band. The transition rate for $a - b$ or $b - a$ is proportional to the probabilities that the state a and b will be occupied times the probability that b (or a) will be empty and thus will accept the electron after it has interacted with the photons. As described, with increasing temperature, $f_c(1 - f_v)$ increases and $f_v(1 - f_c)$ decreases. With any decrease in temperature, f_c increases and f_v decreases, so the gain factor, which according to the Equation 3 depends on $f_c - f_v$, shows a rapid increase with respect to this parameter. Also, the gain peak is shifted toward higher reduced-mass energy. Looking at these figures, it is noted that the peak values for each curve is determined by the condition $d\alpha/d\delta = 0$.

In summary, two major points can be drawn from this analysis. First, the major parameters which control the gain profile are material type and characteristics, band gap, carrier density and temperature. Second, among the parameters studied, lattice temperature plays the most important role in the gain profile and performance of such semiconductor lasers.

ACKNOWLEDGMENT

This work was supported in part by Sharif University of Technology research program. The author gratefully acknowledges the grant devoted to this research. He also acknowledges the technical assistance, concerning some of the numerical computations provided during this study.

REFERENCES

1. Kirby, P.A. "Semiconductor laser sources for optical communications", *Radio Electron. Eng., JIERE*, **51**, pp 363-376 (1981).
2. Hirao, M., Mizuishi, K. and Nakamura, M. "High-reliability semiconductor lasers for optical communications", *IEEE J. on Selected Areas in Commun., SAC-4*(9), pp 1494-1501 (1986).
3. Le Garrerc, B.J., Raze, G.J., Thro, P.Y. and Gilbert, M. "High-average-power diode-array-pumped frequency-doubled YAG laser", *Opt. Lett.*, **21**, pp 1990-1992 (1996).
4. Lerner, E.J. "Diode lasers offer efficiency and reliability"; *Laser Focus World*, pp 93-98 (March 1998).
5. Verdeyen, J.T., *Laser Electronics*, Chap. 11, Prentice-Hall Int., New Jersey (1995).
6. Thompson, G.H.B., *Physics of Semiconductor Laser Devices*, Chap. 2, John Wiley & Sons, UK (1988).
7. Shur, M., *Physics of Semiconductor Devices*, Chap. 5, Prentice-Hall, New Jersey (1990).
8. Meystre, P. and Sargent III M., *Elements of Quantum Optics*, Chaps. 5 and 6, Springer-Verlag, Berlin (1991).
9. Vahala, K., Chiu, C., Margalit, S. and Yariv, A. "On the linewidth enhancement factor α in semiconductor injection lasers", *Appl. Phys. Lett.*, **42**, p 631 (1983).
10. Casey, Jr. H.C. and Stern, F. "Concentration dependent absorption and spontaneous emission in heavily doped GaAs", *J. Appl. Phys.*, **47**, p 631 (1976).
11. Yariv, A., *Optical Electronics*, 4th Ed., Holt, Rinehart and Winston, New York, p 564 (1985).
12. Ahan, D. and Chuang, S.L. "Optical gain and gain suppression of quantum-well lasers with valence band mixing", *IEEE J. Quantum Electron*, **QE-26**(1), pp 13-24 (1990).
13. DeTemple, T.A. and Herzinger, C.M. "On the semiconductor laser logarithmic gain-current density relation", *IEEE J. Quantum Electron*, **QE-29**(9), pp 1246-1252 (1993).
14. Yan, R.H., Corzine, S.W., Coldren, L.A. and Suemune, I. "Corrections for gain in GaAs", *IEEE J. Quantum Electron*, **QE-26**(2), pp 213-216 (1990).